

~~CONFIDENTIAL~~

JAN 16 1952



3 1176 00079 7275

UNCLASSIFIED

NACA

# RESEARCH MEMORANDUM

AN INVESTIGATION OF PROPELLER VIBRATIONS

EXCITED BY WING WAKES

By W. H. Gray and William Solomon

Langley Aeronautical Laboratory  
Langley Field, Va.

CLASSIFICATION CANCELLED

FOR REFERENCE

Authority NACA R. 7 2686 Date 10/12/54

By mda 11/9/54 See \_\_\_\_\_

NOT TO BE TAKEN FROM THIS ROOM

CLASSIFIED DOCUMENT

This material contains information affecting the National Defense of the United States within the meaning of the espionage laws, Title 18, U.S.C., Secs. 793 and 794, the transmission or revelation of which in any manner to unauthorized person is prohibited by law.

## NATIONAL ADVISORY COMMITTEE FOR AERONAUTICS

WASHINGTON  
January 10, 1952

UNCLASSIFIED

~~CONFIDENTIAL~~

NACA LIBRARY  
LANGLEY AERONAUTICAL LABORATORY  
Langley Field, Va.

NACA RM L51G13

UNCLASSIFIED

1W

NACA RM L51G13

~~CONFIDENTIAL~~

NATIONAL ADVISORY COMMITTEE FOR AERONAUTICS

RESEARCH MEMORANDUM

AN INVESTIGATION OF PROPELLER VIBRATIONS

EXCITED BY WING WAKES

By W. H. Gray and William Solomon

SUMMARY

The principal variables affecting the excitation of a propeller for vibration at a frequency of twice propeller speed were investigated using a conventional propeller with solid aluminum-alloy blades operating in the wake of a wing. The drag of the wing was made adjustable through a wide range by the use of 35-percent-chord flaps of the split, the double split, and the aerodynamically balanced types. The spacing between the flap trailing edge and the propeller plane was made adjustable to investigate the effects of wake width and intensity.

The vibratory stress was directly proportional to the free-stream velocity for a fixed value of the wing drag coefficient and varied linearly with the wing drag coefficient for a fixed free-stream velocity. The magnitude of these vibratory stresses was dependent upon the blade damping and the probable mutual interference between the wing and the propeller-blade flow fields. When the vibratory stresses were reduced by the resonant amplification factor (for an assumed single degree of freedom) to equivalent nonresonant stresses, these nonresonant stresses were found to increase with reduced spacing for a given wing configuration and airspeed.

INTRODUCTION

Propeller installations of the pusher type promise alleviation of the wing-flow-disturbance problem inherent in the conventional tractor installation. The pusher installation introduces other problems: the most prominent and undesirable is that of propeller vibrations resulting from the blade passage through the variable-velocity flow field in the wake of the wing. A blade encounters this flow field twice per revolution. Resonance occurs, therefore, when the natural frequency of the rotating blades is equal to twice the frequency of rotation. Should the aerodynamic forces on the blades arising from the wing wake be of sufficient

~~CONFIDENTIAL~~

UNCLASSIFIED

magnitude, the blades may operate under conditions of excessive stress, particularly if resonance occurs. Blade failures have occurred under service conditions with airplanes employing propellers behind control surfaces.

A series of pusher-propeller vibration tests was conducted previously in the Langley 16-foot high-speed tunnel (reference 1) and an analysis of the data together with considerations of wing-wake excitation of a propeller blade has been presented in reference 2. Based on an equation derived from simple blade-element theory, the principal conclusions of this analysis were that the intensity of the wake-excited periodic forces acting on the blade of a pusher propeller varies directly with air density, airspeed, propeller rotational speed, and drag of the body producing the wake. The limited amount of data then available appeared to bear out the conclusions.

Because of the limited amount of data then available and the desirability of obtaining a better check on the theory, an additional program was initiated at the Langley 16-foot high-speed tunnel. The program was intended to cover a wide range of wing drag coefficients and to establish the comparative effect upon blade stresses of wake intensity and wake width for the same drag coefficient. Also, to provide for better design of propellers for pusher installations, a study was planned to evaluate the magnitude of the constants of the equations derived in reference 2 for the vibratory exciting force using the results of the test program. The propeller assembly was chosen to correspond, as nearly as possible, to a conventional installation using an electric hub so that blade flexibility and blade retention would be duplicated.

#### SYMBOLS

The symbols and definitions used in the present paper are as follows:

- a value of rotational correction factor,  
1.7 herein
- B number of blades
- b blade chord, feet
- $C_1, C_2, C_3$  constants of exciting-force equation
- c wing chord, feet
- $c_l$  section lift coefficient

$c_{l_d}$	design section lift coefficient
$C_P$	power coefficient $(P/\rho n^3 D^5)$
$C_T$	thrust coefficient $(T/\rho n^2 D^4)$
D	propeller diameter (10.0 ft)
h	blade section maximum thickness, feet
J	advance ratio $(V/nD)$
k	order of propeller excitation frequency, 2 herein
L	lift, pounds
$\Delta L$	propeller blade vibratory exciting force, pounds
M	bending moment, foot-pounds
m	slope of lift coefficient curve (5.73/radian, assumed)
N	propeller rotational speed, rpm
$N_0$	rotational speed at resonance, rpm
$\Delta N$	difference between two rotational speeds at which stress is 0.707 of magnitude at resonance, rpm
n	propeller rotational speed, rps
P	power absorbed by propeller, foot-pounds per second
R	propeller tip radius (5.0 ft)
T	propeller thrust, pounds
V	free-stream airspeed, feet per second
z	section modulus, feet <sup>3</sup>
x	fraction of propeller tip radius
$\beta$	blade angle, degrees

$\rho$  air density, slugs per cubic foot  
 $\sigma$  stress, pounds per square foot

#### APPARATUS AND METHODS

Dynamometer and wing.- These propeller tests were designed to utilize the NACA 2000-horsepower propeller dynamometer as the test vehicle. A complete description of this dynamometer and the method of measuring propeller forces may be found in reference 3. A five-foot chord, 15-foot span wing, with an NACA 66<sub>1</sub>-012 airfoil section was installed in front of the dynamometer and at thrust-axis level (figs. 1 and 2). Provision was made for the installation of single split, double split, and aerodynamically balanced flaps, each of which had a chord of 21 inches. The flaps extended from each tunnel-end-plate to the surface of the 26-inch-diameter fairing which served to house the propeller hub, strain-gage wiring, and slip-ring device. A wide range of flap angles was obtained with the single- and double-split flaps by the use of wedges between the upper and lower surfaces. The balanced flap was clamped at angles from 0° to 20°. No flap nose gap seal was provided for the balanced flap except for the 20° deflected flap position, for which deflection it was noted that there was intermittent flow through the slot as indicated by alternate increase and decrease of the drag measured by wake survey. The gap was therefore sealed on the upper surface for all 20° deflection tests with propeller operating.

The wing and fairing to the propeller spinner was maintained in a freely floating condition with respect to the tunnel wall at all times, restrained only by the tunnel balance system which measured the forces on the model independent of the propeller forces. So that the effect of leakage through the tunnel wall would be a negligibly small factor, the wing was mounted on 5-foot-diameter end plates integral with the tunnel balance frame. (See fig. 1.) These end plates minimized any tendency for changes in end-plate tare or for influencing wing drag.

In order to maintain the drag coefficient of the wing at 0° flap angle essentially constant regardless of surface conditions, a transition strip  $\frac{1}{2}$ -inch wide composed of 0.011-inch carborundum particles was attached to the wing at the 23-percent-chord location. As the wing was operated only at 0° angle of attack and the leading edge was quite smooth, it was assumed the transition would not have occurred at least until the quarter-chord point had been reached.

Survey rake.- The wake survey rake consisted of a bank of 50 total pressure tubes and nine static tubes. As the wing was operated only at  $0^\circ$  angle of attack, the rake was maintained at all times in a vertical position.

Propeller.- The 10.0-foot-diameter propeller used in these tests employed a standard three-way electric hub. Because of the procedure used in running these tests, it was necessary to have the blade angles continually adjustable.

The blades were Curtiss solid aluminum-alloy blades designated 109392 and have the characteristics shown in figure 3. The activity factor was 120 per blade. The blades were chosen to have a resonant frequency for excitation at twice the propeller speed ( $2N$ ) within the rotational speed range of the dynamometer. The static natural frequency in first bending mode flatwise was 27.0 cycles per second with the hub fixed. If the centrifugal correction factor for the first bending mode is assumed to be 1.7 (reference 4) the resonance prediction curve for this mode is that shown in figure 4. Resonance should occur at the intersection of the  $2N$  and natural frequency curves at 1060 rpm. Actually resonance occurred at about 1000 rpm which indicated slight changes in either the centrifugal correction factor or the static natural frequency or both.

Instrumentation.- The propeller blade stresses were measured with wire strain gages, the gage installation being shown in figure 5. Blade A carried a radial wire strain gage ( $S_A$ ) on the blade camber face at the 0.75-radius station as well as straight gages placed in supplementary pairs at angles of  $0^\circ$ ,  $45^\circ$ , and  $90^\circ$  around the shank. A rosette gage ( $RA$ ) was also attached to the camber face of this blade at the 0.55 radius station. On blade B was attached a straight gage at the 0.55 radius station ( $S_B$ ) in order that the phasing of the vibratory stresses of blades A and B might be compared. The purpose of the installation of the rosette on blade A was to enable the determination of the direction as well as magnitude of the principal stress. Some doubt had been expressed that the principal stresses were radial even on the solid metal blades.

The schematic wiring diagram of the strain-gage installation for measurement of propeller stresses is given in figure 6. Except for the shank gages only one gage, or one arm of a bridge, was installed on the blade, which necessitated the use of a dummy arm or fixed resistance, for a second arm. These fixed resistances were located as near as possible to the active arms, at the blade shank. The remaining two arms of the bridges were two dummy gages which were common to all, including the paired shank gages. The combination of the low output voltage of the gages and the low sensitivity of the oscillograph elements necessitated the use of amplifiers between the bridges and oscillograph. At least

two calibrations were taken on each amplifier-oscillograph channel used in each run. The latter procedure necessitated the use of the oscillator and millivoltmeter shown in the diagram; the known calibrating voltage was applied at a known frequency which closely approximated that obtained at resonance for these tests. A simple ratio of known applied calibration voltage, comparative magnitude of calibration record, and operating stress record magnitudes gave the value of the bridge output voltage, or the stress equivalent.

The auxiliary oscillograph enabled observation of the functioning of the strain gages and slip rings as well as providing a check on the total (vibratory plus steady) blade stresses during operation.

### TESTS

Profile-drag surveys.- The profile-drag surveys were made in the absence of the propeller with the wake survey rake placed behind the wing at a spanwise position representing the 0.7 radius (42-in.) station on the blade, because it seemed reasonable to assume, as had been assumed in reference 2, that the 0.7-radius blade station was a representative station, and because the wing producing the exciting force was of constant chord spanning the tunnel jet. Wake surveys were made in a vertical plane 42 inches to the left of midspan at downstream distances corresponding to a spacing of the plane of rotation of the propeller center line; 9, 18, and 30 inches (15, 30, and 50 percent of the wing chord, respectively) behind the trailing edge of the wing at zero flap angle. The range of flap angles and velocity used with each of the three flap types during the survey runs is shown in table I.

Wing-force data.- Concurrently with the wake-survey measurements, the drag characteristics of the wing-fairing assembly were obtained with the tunnel scale system. The model construction and arrangement permitted the drag of the wing-fairing assembly to be checked with propeller operating. However, it was necessary to apply several corrections to the measured drag forces.

The major correction applied was a result of the pressure field in the wake of the wing-fairing assembly. This pressure was transmitted inside the fairing ahead of the propeller spinner, and the difference between this internal pressure and the free-stream static pressure produced a force measurement on the drag scales. The difference in pressure was measured and the necessary corrections to account for this pressure force were applied to all the drag-coefficient data presented.

Although the foregoing correction was a variable with flap type and flap angle, the other corrections applied were constants. These

include skin friction on the fairing which yielded a drag coefficient related to wing area of 0.002, tare drag of the end plates alone which yielded a drag coefficient based on wing area of 0.001 and a buoyancy correction which was negligible. Only the drag caused by interference between the flap and fairing and between the flap and end plates could not be evaluated. It is believed that the interference between the flap and fairing constitutes a part of the propeller exciting force in addition to the normal wing wake.

Propeller operating regime for vibration tests.- The propeller operating conditions were selected from considerations of the requirements of the vibration tests as indicated in the equation derived in reference 2. This equation gives the magnitude of the propeller-blade vibratory exciting force  $\Delta L$  as follows:

$$\Delta L = C_3 \frac{\rho n D^3}{4} \left[ m \pi C_2 - \frac{64}{\pi^2 B} \frac{C_1}{(b/D)_{0.7R}} \frac{C_{TJ}}{\sqrt{J^2 + 4.84}} \right] V \quad (1)$$

The terms  $C_1$  and  $C_2$  are based only on geometric characteristics of the blades:

$$C_1 = \int_{0.2}^{1.0} \frac{b}{D} dx = 0.0642 \quad (2)$$

$$C_2 = \int_{0.2}^{1.0} \frac{b}{D} x dx = 0.0390 \quad (3)$$

$B$ ,  $(b/D)_{0.7R}$ ,  $D$ , and  $m$  are constants for any given set of blades.

The term  $C_3$  is based on the velocity change in the wake of the wing effective in producing the vibratory exciting force. At all positive values of thrust coefficient, the magnitude of the blade vibratory exciting force would be reduced by the value of the second term, in brackets, of equation (1). For the purposes of simplifying the present tests, therefore, the majority of the runs were conducted at zero power which was the best means of setting a value of  $C_T$  very close to zero.

With the second term of the expression zero, the equation for the vibratory exciting force reduces to

$$\Delta L = 1.75 \rho n (C_3 V) \quad (4)$$

It can be seen from equation (4) that testing would be further simplified by maintaining constant velocity. A velocity of 150 miles per hour was

chosen because at this velocity the desired range of rotational speed could be encompassed at zero power within the controllable blade-angle range of the propeller. Except for the tests at 0° flap angle for which the velocity was varied from 120 to 350 miles per hour, the test program (table I) was restricted to 150 miles per hour. Records were obtained at sufficiently small intervals of rotational speeds over the range from 400 to about 1350 rpm to define the propeller vibratory response curve.

Sufficient aerodynamic propeller data were taken during the tests to insure that the propeller was operating within reasonable limits of the required value of constant power coefficient.

## RESULTS AND DISCUSSION

### Wing Drag Data

Wing drag coefficient as defined by faired values of the force measurements are utilized in the presentation of the vibratory stress results in the present paper. The force measurements are used because no valid picture of the wing drag could be obtained from the wake survey at only one spanwise station. The variation of wake width with flap angle, the variation of force drag coefficient with flap angle, and the variation of wake width with force drag coefficient are shown in figures 7, 8, and 9 in order to provide some idea of the quantities obtained with each configuration.

### Vibratory Stresses

The gage designated  $R_A$  was located at what was estimated from a preliminary shaking to be the point of maximum blade vibratory stress for the first bending mode. A comparison of the stresses from the  $R_A$  gage with the stresses at the other gage locations indicated that the stresses at  $R_A$  were actually greatest, and since a complete blade stress distribution was not needed to arrive at the conclusions of the present paper, only these maximum measured stress data are presented.

In order to compare the experimental results with theory, it was necessary to determine the 2N component of the recorded stress values by harmonic analysis. The 2N analyzed component of the recorded stresses is shown for a typical response curve in figure 10. Because the desired comparisons for this paper are obtained for a resonant condition, the assumption is made that the maximum 2N analyzed stress is the maximum that occurs at resonance, although it is realized that there will be a resulting scatter of the data presented because of the inability to

space the test points close enough to determine resonance precisely. All stress values presented therefore are the maximum  $2N$  stress components determined from harmonic analysis of the recorded stress values for the  $R_A$  gage.

For the solid aluminum-alloy blades tested, the principal stresses computed from the rosette gage were radial. The straight gage  $S_B$  which was mounted on another blade at the same radial station as the rosette  $R_A$  indicated approximately the same stress level and a phase difference equal to the  $120^\circ$  angular difference between the respective blades. The shank gages verified that resonance occurred in the first flatwise bending mode. It should be noted that whereas the resonant  $2N$  propeller stress data in previously published literature are largely for the edgewise mode, the stress data reported herein are for the flatwise bending mode. The difference may be explained by a consideration of the blade natural frequencies in the flatwise and edgewise modes and the relationship of these frequencies to the operating range of the test vehicle.

Effect of blade angle on resonant frequency. - Neither the bench tests to determine the static natural frequency nor previously published data had indicated conclusively that blade angle has any effect on the resonant frequency. It seemed reasonable that the individual hub barrels might be weaker (that is, the blade would have less restraint and a lower natural frequency) when the blade was vibrating in a bending mode perpendicular to the plane of the hub. Such a condition would mean that the resonant frequency for flatwise bending would increase with increasing blade angle. In the present tests the maximum deviation found in the resonant frequency for five separate runs in which the blade angle was changed in  $5^\circ$  increments from  $20^\circ$  to  $40^\circ$  at the 0.75 radius station was 18 rpm or 1.8 percent. There was no consistent effect of blade angle on the average resonant speed of 1000 rpm.

Effect of power on peak stress. - Although it was not anticipated that there would be any change in the resonant frequency at various powers, some change in peak stress at resonant frequency might be expected. The blade angle could not be maintained constant for these runs as they were made at constant tunnel velocity, but varying rotational speeds. Therefore the runs were made in a manner similar to that adopted for determining the response curves. At two different values of constant tunnel velocity the rotational speed was varied through as wide a range as possible within the limits of 400 and 1350 rpm and data were taken at each rpm for the five values of power coefficient,  $C_p$  of 0, 0.05, 0.10, 0.15, and 0.20. Inasmuch as it had already been established that blade angle had no effect on resonant speed, then for the resonant speed

of 1000 rpm at constant tunnel speed, the change in power would be proportional to the change in the power coefficient. Power coefficient was the criterion used because of the ease of its determination and control during the test.

A scatter of peak stress values of about 10 percent was found which, however, could not be resolved into any specific trend. It was concluded, therefore, that there was no effect on the peak resonant stresses caused by a variation in the propeller power, for the range investigated.

As a consequence of the two preliminary investigations described above, which were made with the propeller 30 percent of the wing chord behind the zero angle flap, the remaining and principal parts of the investigation were conducted at zero power (and there was no attempt made to record the blade angle).

Effect of velocity and drag on resonant stress.- Elementary theory (reference 2) indicates that the intensity of the wake-excited periodic forces causing the vibratory stresses in the blades should be proportional to air density, to airspeed, to propeller rotational speed, and to the drag of the body producing the wake. For a fixed value of drag coefficient (flap at  $0^\circ$  angle) and spacing, the vibratory stress varies directly with airspeed (fig. 11). This effect may be expected from equation (4) because resonance always occurred at essentially the same value of rotational speed. Two separate lines define the variation of stress with velocity in figure 11, one for the 0.50-chord spacing and one for both the 0.15- and 0.30-chord spacings, the latter having about twice the slope of the former. The relation derived in reference 2 is for the incompressible case, and it is not expected that the linearity would be maintained above the relatively low velocities investigated. Stresses higher than those predicted by an extrapolation of the linear fairing should be encountered at higher velocities because of the increased lift-curve slope with Mach number until a portion of the outer blade sections has reached the section lift force-break Mach number. At even higher velocities, above the section lift force-break Mach number, lower stresses than predicted by linear extrapolation may be encountered.

Figure 12 shows the effect (at a velocity of 150 mph) of the drag coefficient of the wake-producing body upon vibratory stress. Here again the linear variation of stress with drag coefficient predicted by theory is verified by the experimental results. For the 0.15- and 0.30-chord spacings the stress variation with wing drag coefficient is about the same as for the 0.50-chord spacing but the stress magnitudes are greater over the entire range by about 1200 psi.

An explanation of the coincidence of the stress values for the 0.15- and 0.30-chord spacings is found by a study of the relative amounts of damping present for the three spacings. The stresses presented, because

they are resonant stresses, are affected considerably by the amount of damping in the system. The damping factors, or ratios of the actual damping to critical damping, have been evaluated by the following method. It may be shown that the value of the damping factor may be obtained from the spread of the response curve at 0.707 of the resonant curve amplitude. (See reference 5.) For a rotating propeller blade with small damping the relationship takes the form:

$$\text{Damping, fraction of critical} = \frac{\Delta N}{2N_0} \left( 1 - \frac{a}{k^2} \right)$$

This factor includes all the elements producing damping of the blade vibrations, aerodynamic as well as mechanical. At resonance the amplification of the stress is solely a function of this damping factor and for a forced vibration with a single degree of freedom with damping equals one-half the inverse of the damping factor at resonance. The resonant stresses may therefore be corrected to unmagnified values that are directly comparable. The damping factor at the 0.30-chord spacing was found to be about 70 percent of the factor for both the 0.15- and 0.50-chord spacings. The resulting comparison of unmagnified stress ratio (related to stress at the 0.50-chord spacing) for the balanced flap configuration (see fig. 13) indicates an increase in unmagnified stress with decreased spacing for a given drag coefficient, rather than the coincidence of resonant stress at 0.15- and 0.30-chord spacings shown in figures 11 and 12. The cause of the observed change in the response curve total damping factor with spacing is believed to be aerodynamic. Mechanical changes in blade retention do not appear to be a contributing factor because changes in spacing were accomplished by movement of the independently mounted wing rather than by movement of the dynamometer.

The reason for a stress increase with decreased spacing is not predicted by simplified theory. In the simple theory of reference 2, there is considered to be no difference in stress with spacing at constant drag coefficient, because the narrow intense velocity defect close to the wing was expected to provide the same excitation impulse as a broader, less intense velocity defect further downstream. One factor which may have caused this augmentation of stress with reduced spacing is that the increased proximity of the wing with smaller spacings resulted in a mutual interference between the wing and propeller blade pressure fields, which caused a finite rise in stress level. Although this factor might seem to be ruled out by the fact that all the tests were conducted at zero power, at which condition the average thrust coefficient over the blade was very nearly zero, the actual lift coefficients of the blade sections varied from negative to positive in each half cycle of rotation and appreciable interference might have occurred. Although

this effect is possible, it cannot be proven because changes in the energy of the wake ahead of and behind the propeller would have had to be measured.

### Theoretical Considerations of Wake Excited Blade Stresses

In order to utilize the equations of reference 2 for predicting blade stresses, the factor  $C_3$  (see equation (1)) must be evaluated. The influence upon  $C_3$  of the following parameters must be determined: drag coefficient of the wake producing wing, stream velocity, and wing-propeller spacing. An empirical evaluation of  $C_3$  was one of the objectives of this investigation. Attempts at an evaluation were made considering in one case the experimental stress results and in a second case the axial-velocity field which the blade traverses each cycle (fig. 14). In the process of analysis it was found that the system damping exerted a major influence upon the results (see appendix). Because an explanation of the measured damping level and of the effect of spacing upon damping could not be ascertained, it was not considered possible to utilize the results of the empirical evaluation of  $C_3$  for predicting the blade stresses of any other pusher propeller configuration.

In an effort to determine whether the inadequacy of the approach of reference 2 to predict resonant blade stresses was caused by possible oversimplification of the aeroelastic problem, a third attempt at computing blade stresses was made. This latter analysis considered the blade as an elastic body subjected to periodic gust-type loads exerted by the blade passage through an axial velocity field such as is shown in figure 14. However, this approach, which included the aeroelastic effect and which required no initial assumptions about the system damping level, gave no better results than the simple analyses. A better understanding of the mechanism of blade response to the very short periodic sharp-gust-type load at the resonance condition is needed in order to utilize this aeroelastic method of analysis.

The need for more extensive knowledge of the effect of the various aerodynamic and structural parameters upon blade response and system damping deterred the use of the data of this investigation for a theoretical evaluation of resonant wake-excited blade stresses.

### SUMMARY OF RESULTS

The results obtained from the data and the data analysis may be summarized as follows:

1. The vibratory stress was directly proportional to the free-stream velocity for a fixed value of the wing drag coefficient at a

given spacing. The magnitude of this stress was dependent upon the blade damping and the probable mutual interference between the wing and the propeller blade flow fields.

2. A linear variation of stress with drag coefficient for a fixed velocity was measured. The two closer spacings (0.15-chord and 0.30-chord) gave coincident values of stress at a given drag coefficient which were higher than those obtained for a spacing 0.50 wing chord behind the wing trailing edge. These values also were functions of blade damping and probable mutual interference between the wing and the propeller-blade flow fields.

3. When the vibratory stresses were reduced by the resonant amplification factor (for an assumed single degree of freedom) to equivalent nonresonant stresses these nonresonant stresses were found to increase with reduced spacing for a given wing configuration.

4. An explanation of the effect of wing trailing-edge - propeller spacing upon damping is necessary for a theoretical evaluation of wake-excited resonant blade stresses.

5. There was no effect of blade angle on resonant frequency.

Langley Aeronautical Laboratory  
National Advisory Committee for Aeronautics  
Langley Field, Va.

## APPENDIX

EXPERIMENTAL DETERMINATION OF  $C_3$  FACTOR

## IN EXCITING FORCE EQUATION

The relations used to evaluate  $C_3$  from the experimental stress results evolve from the expression given in reference 2 relating the change in lift over the propeller blade to the change in axial velocity:

$$d \left( \frac{dL}{dV} \right) = \rho \frac{D^2}{4} \left( 2Vc_l \frac{b}{D} dx - m\pi n D x \frac{b}{D} dx \right) \quad (A1)$$

Normally for these tests the term containing  $c_l$  is small compared with the second term and because the tests were conducted at zero power coefficient (small negative lift coefficient for the propeller blade sections), the term containing  $c_l$  is considered to be negligible. (A calculation of the magnitude of the neglected term for the conditions of these tests justified this conclusion.) The vibratory shear, then, to any radial station  $x$  is given by:

$$\frac{dL}{dV} = - \rho \frac{D^2}{4} m\pi n D \int_x^{1.0} x \frac{b}{D} dx \quad (A2)$$

The vibratory moment to  $x$  follows directly as

$$\frac{dM}{dV} = - \frac{\rho D^3}{8} m\pi n D \int_x^{1.0} \int_x^{1.0} x \frac{b}{D} dx dx \quad (A3)$$

A first approximation to the vibratory stress utilizing only the aerodynamic exciting moment is then

$$\frac{d\sigma}{dV} = \left( \frac{dM}{dV} \right) \frac{1}{Z} \quad (A4)$$

where  $Z$  is the section modulus of the blade section at  $x$ . The substitution of  $C_3 = - \frac{\Delta V}{V}$  with the further stipulation as given in reference 2 that  $dL$  and  $dV$  can be considered finite increments (implying  $dL = \Delta L$  and  $dV = \Delta V$ ) yields an expression for determining to a first approximation the factor  $C_3$  from the experimental stresses:

$$C_3 = \frac{-\Delta\sigma(Z)}{\left(\frac{dM}{dV}\right) V} \quad (A5)$$

where  $\Delta\sigma$  is vibratory stress. Because the level of the damping for this investigation (from  $1\frac{1}{2}$  to 4 percent of critical damping) is a variable, and because damping probably will be a variable in all resonance conditions with pusher installations, the unmagnified value of vibratory stress must be used as  $\Delta\sigma$  in equation (A5). A small error in the determination of the damping factor causes a greatly magnified error in the value of  $C_3$  determined by this method. Also application of the derived values for  $C_3$  to the prediction of stresses in other pusher installations requires an exact knowledge of the damping level and the effect of spacing upon the system damping.

## REFERENCES

1. Miller, Mason F.: Wind-Tunnel Vibration Tests of a Four-Blade Single-Rotating Pusher Propeller. NACA ARR 3F24, 1943.
2. Corson, Blake W., Jr., and Miller, Mason F.: Considerations of Wake-Excited Vibratory Stress in a Pusher Propeller. NACA ACR L4B28, 1944.
3. Corson, Blake W., Jr., and Maynard, Julian D.: The NACA 2000-Horsepower Propeller Dynamometer and Tests at High Speed of an NACA 10-(3)(08)-03 Two-Blade Propeller. NACA RM L7L29, 1948.
4. Theodorsen, T.: Propeller Vibrations and the Effect of the Centrifugal Force. NACA TN 516, 1935.
5. Myklestad, N. O.: Vibration Analysis. McGraw-Hill Book Co., Inc., 1944, p. 111.

TABLE I  
OUTLINE OF INVESTIGATION

Flap configuration	Trailing edge to propeller spacing in wing chords	Flap angles tested (deg)		Velocity (mph)	
		Survey tests	Stress tests	Survey tests	Stress tests
Balanced	0.15, 0.30, 0.50	0	0	120 - 350	120 - 350
	0.15, 0.30, 0.50	0, 5, 10, 15, 20	0, 5, 10, 15, 20	150	150
Single Split	0.15	0, 13, 18, 28, 38	28	150	150
	0.30	0, 13, 18, 28, 38	13, 18, 28, 38	150	150
	0.50	0, 13, 18, 28, 38	18, 28, 38	150	150
Double Split	0.30	<sup>a</sup> 13, 18	<sup>a</sup> 13, 18	150	150
	0.50	<sup>a</sup> 13, 18	-----	150	-----

<sup>a</sup>For double-split flaps the angles are given as degrees per flap.



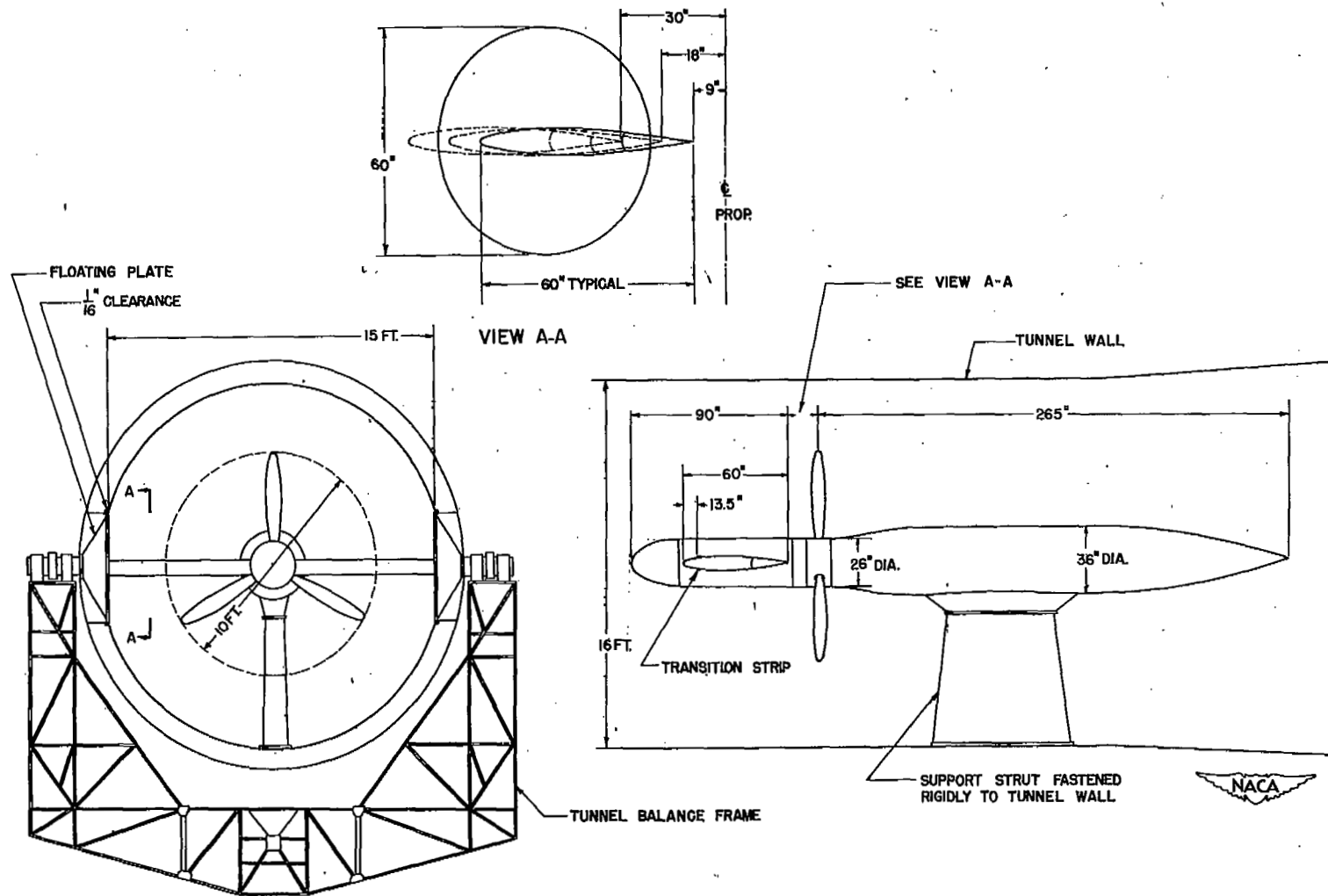


Figure 1.- Configuration for vibration tests of pusher propellers in the Langley 16-foot high-speed tunnel.

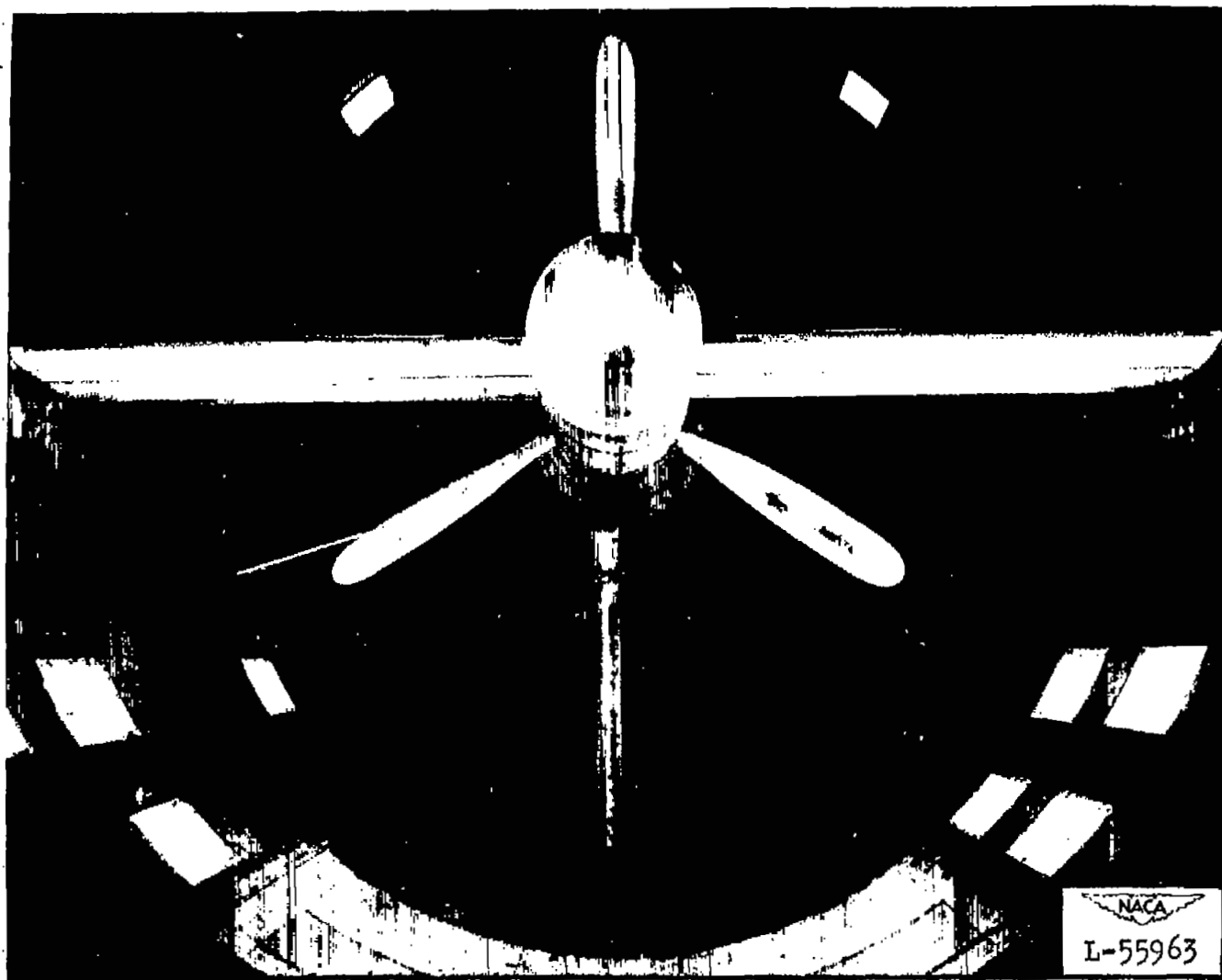


Figure 2.- General view of test arrangement.

# ***Error***

---

An error occurred while processing this page. See the system log for more details.

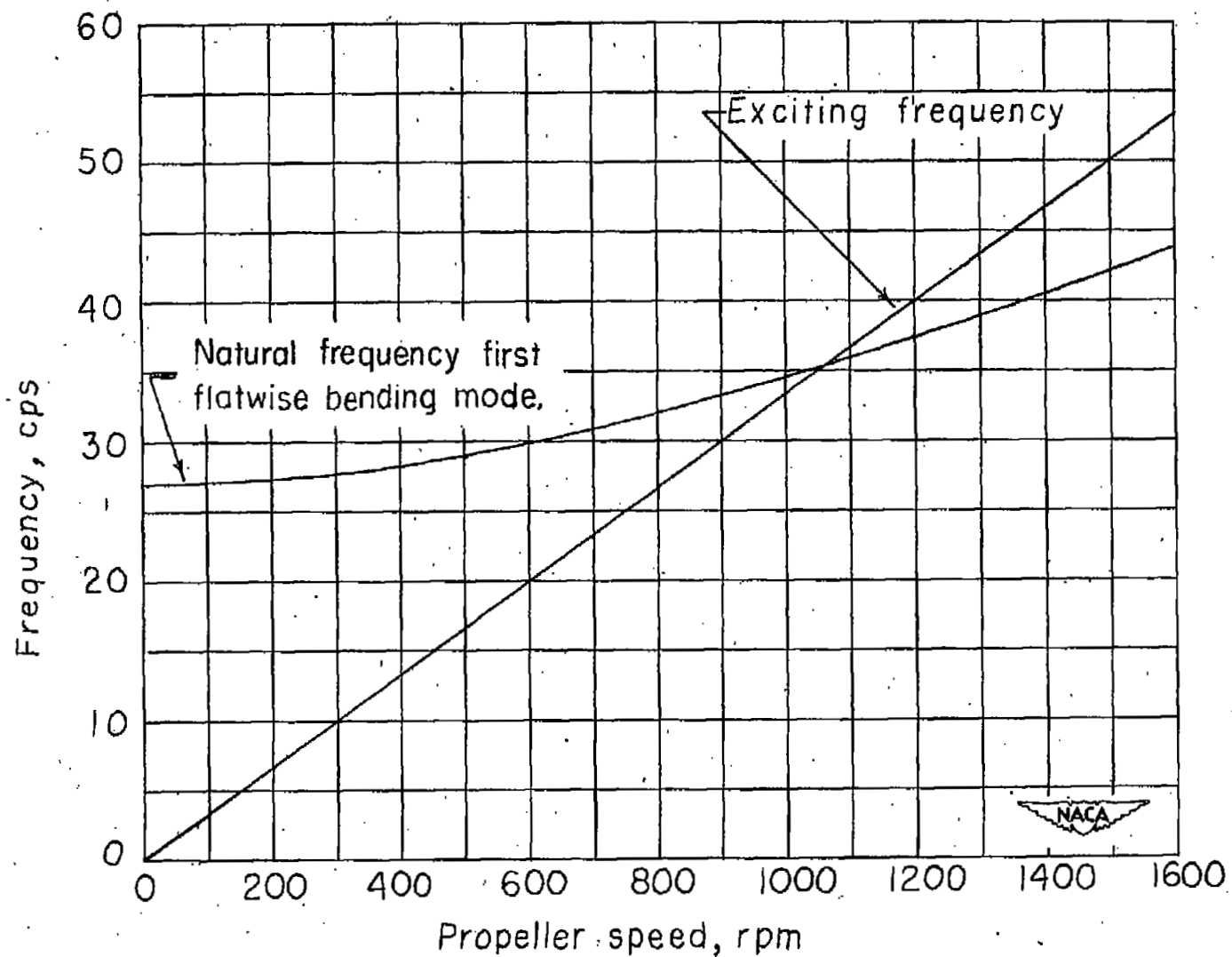
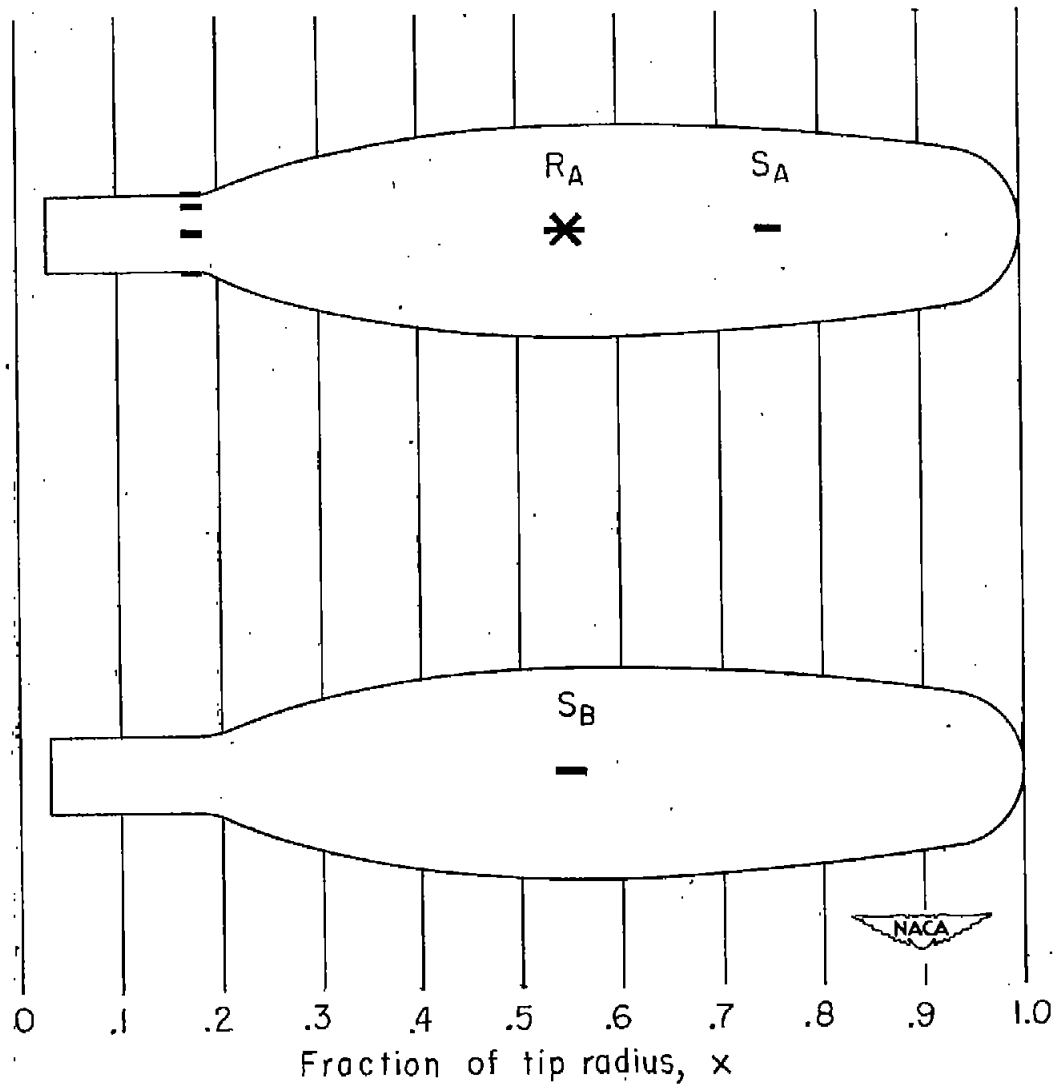
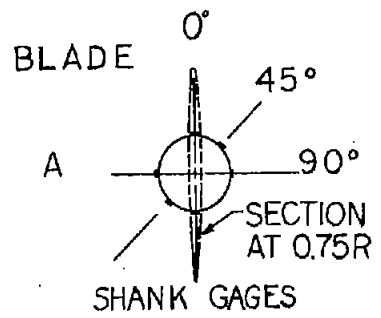


Figure 4.- Prediction of rotational speed at resonance for blade excitation at twice propeller speed.



BLADE  
B

Figure 5.- Diagram of blades showing strain-gage location.

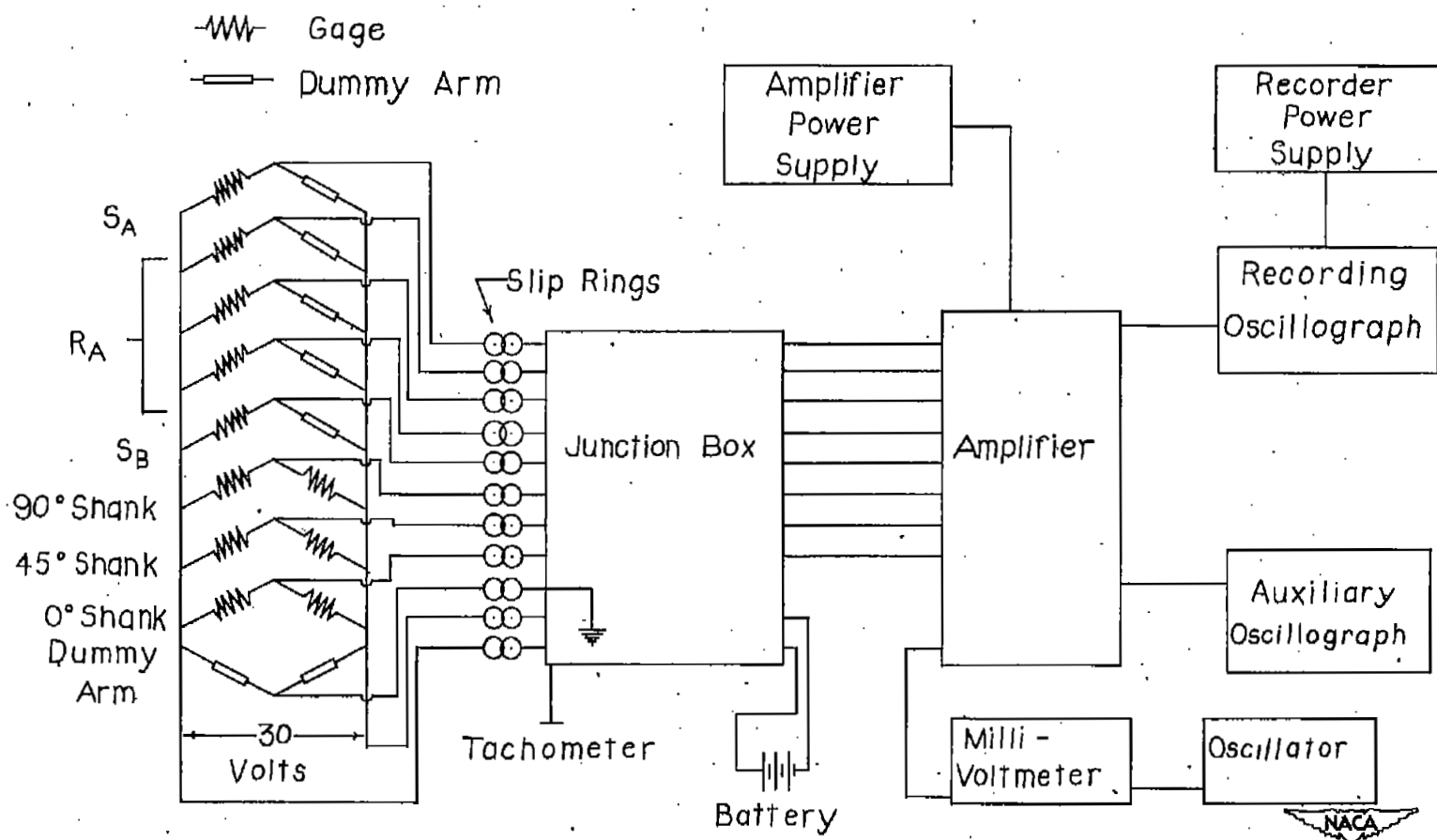


Figure 6.- Schematic wiring diagram.

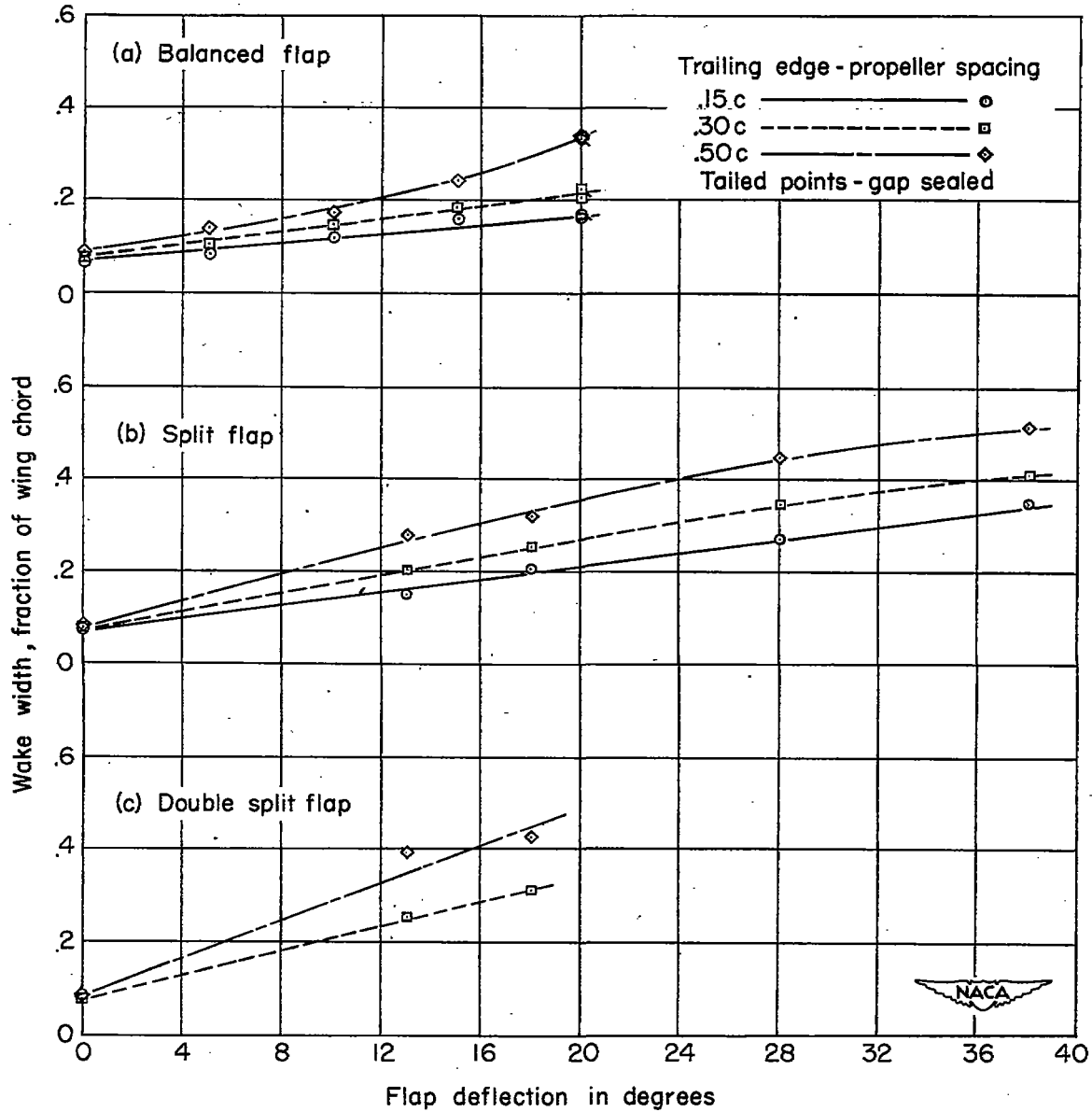


Figure 7.- Wake width as a function of flap deflection angle.

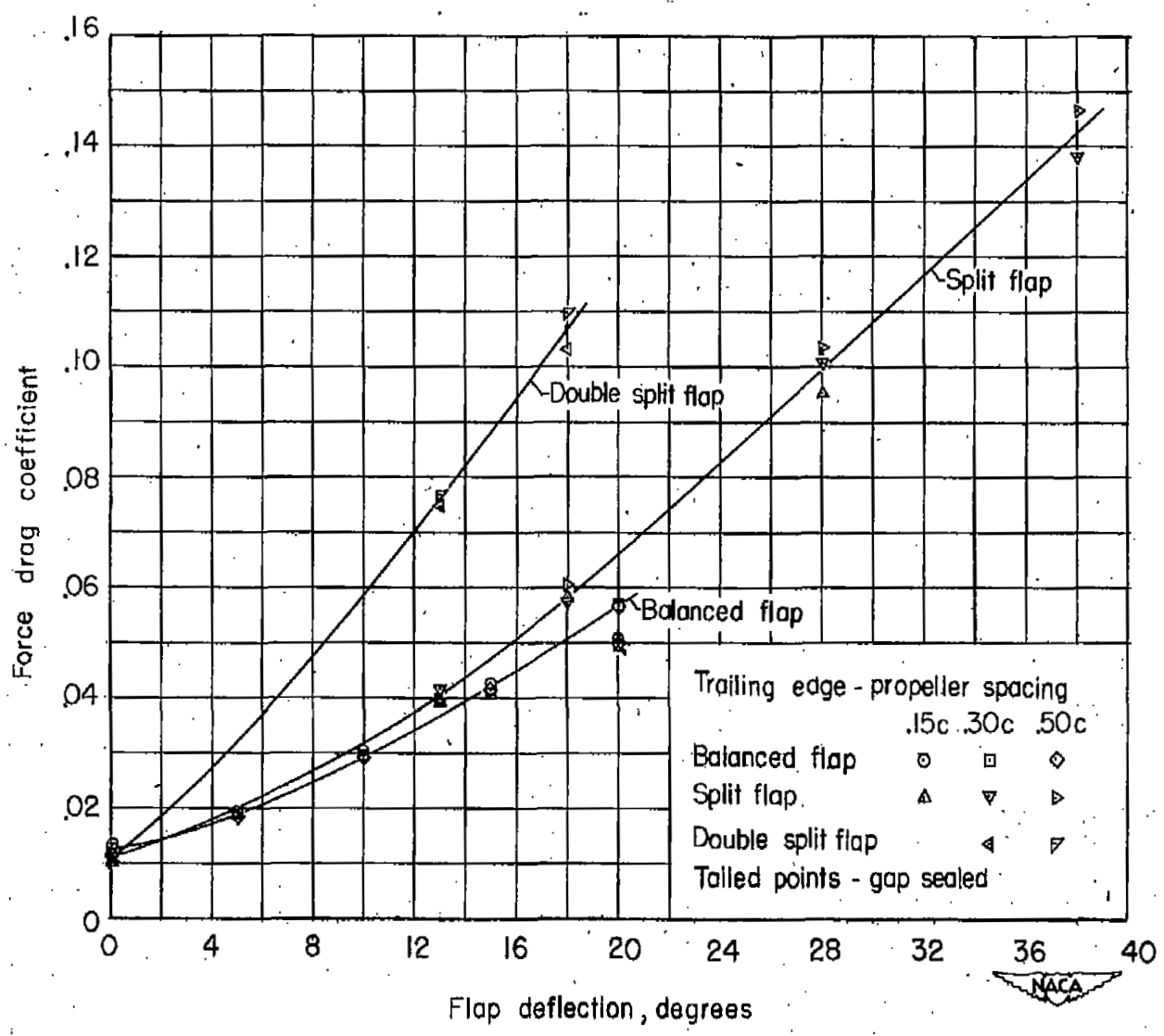


Figure 8.- Force drag coefficient as a function of flap deflection angle.

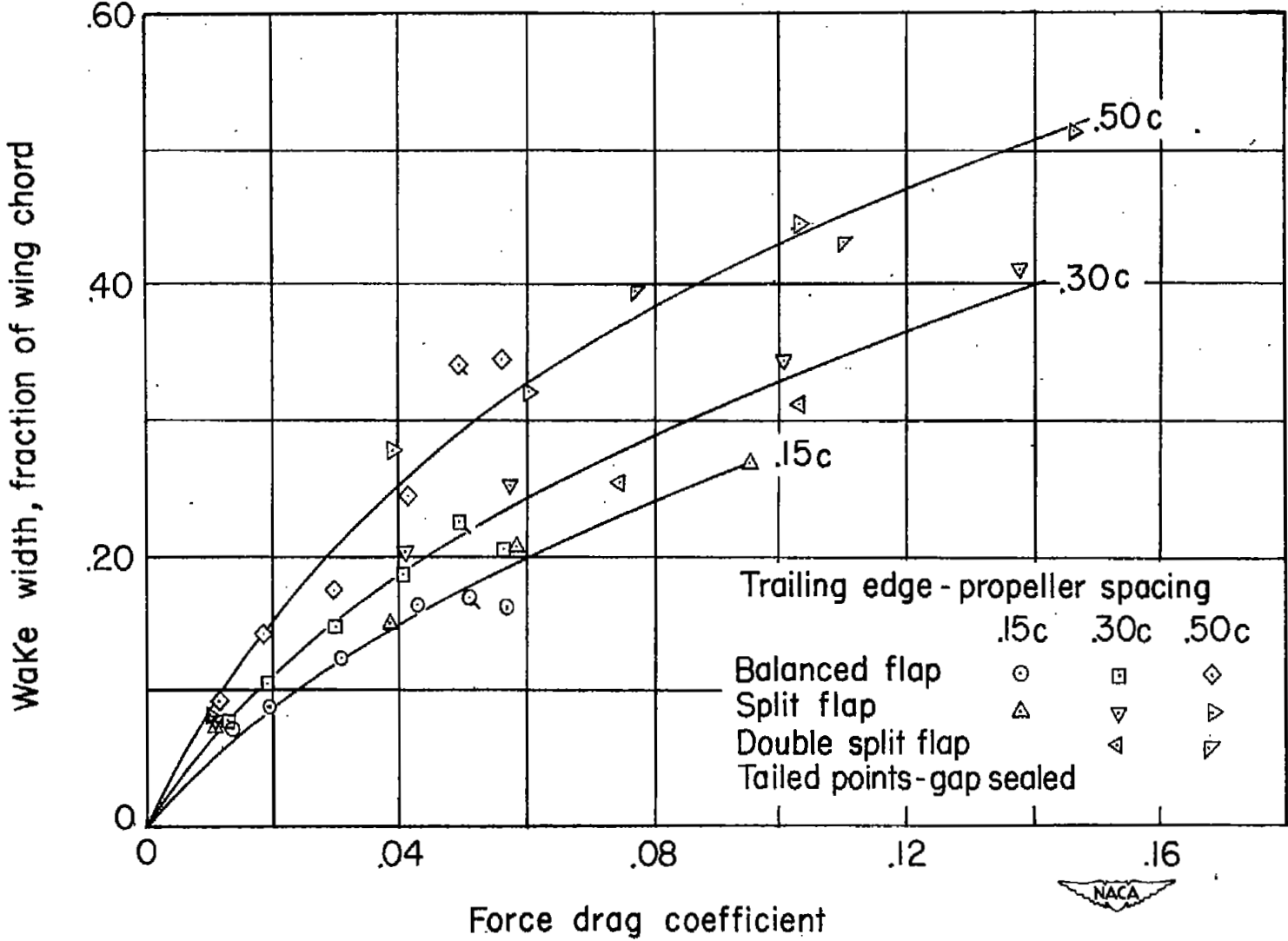


Figure 9.- Wake width as a function of force drag coefficient.

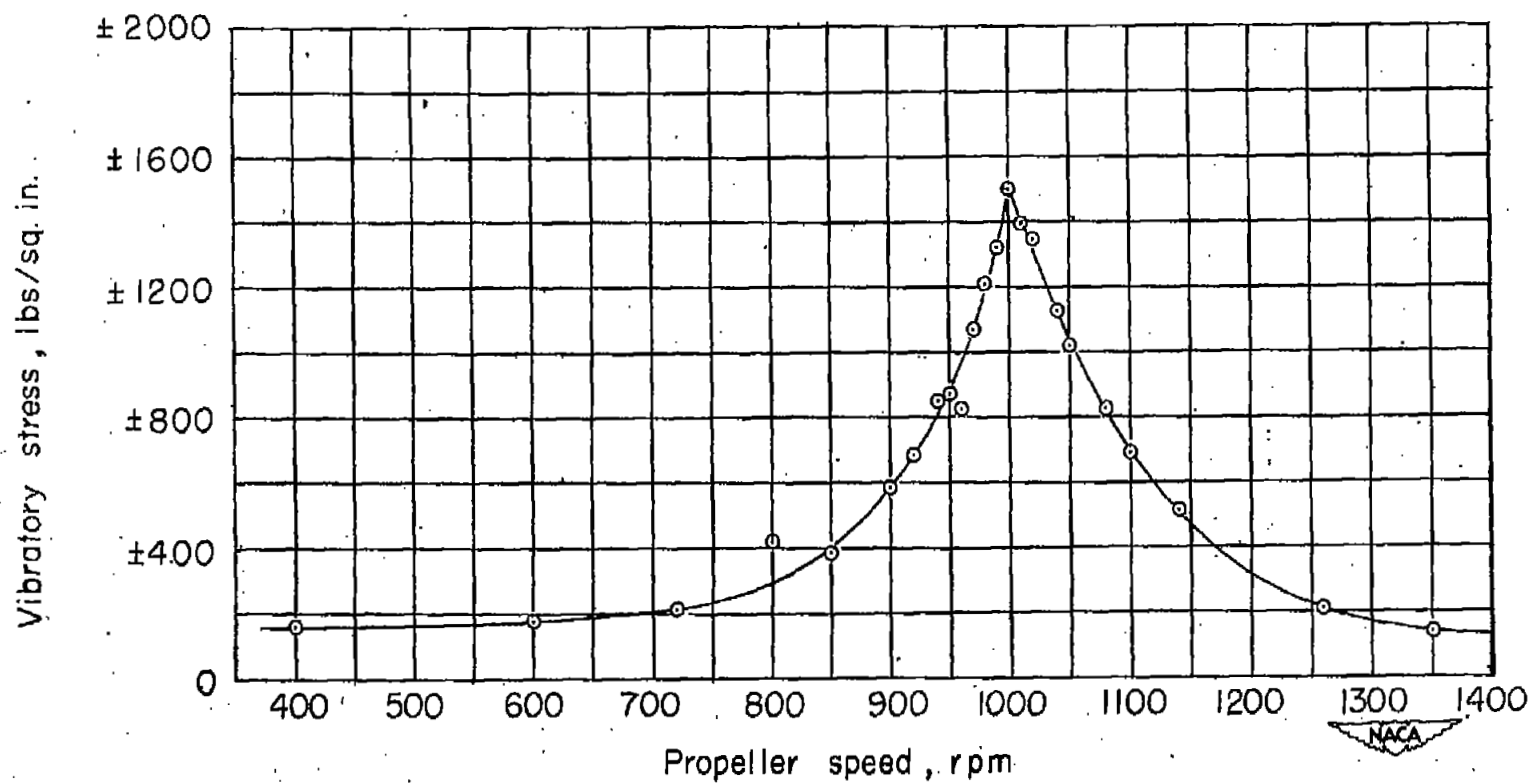


Figure 10.- Sample analyzed vibratory stress response curve;  $R_A$  gage; balanced-flap angle =  $15^\circ$ ; trailing-edge - propeller spacing  $0.50c$ ;  $C_p = 0$ ;  $V = 150$  miles per hour.

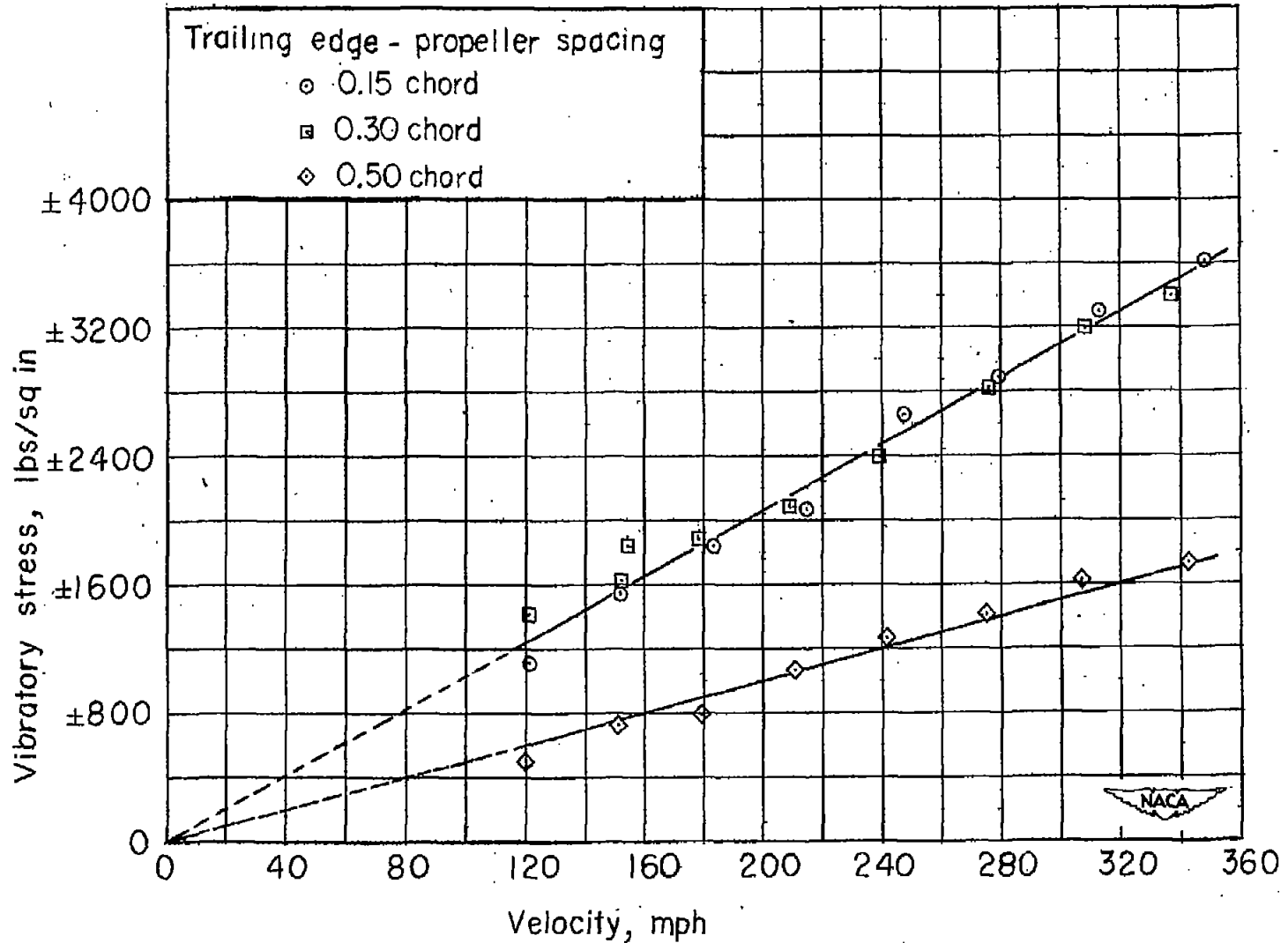
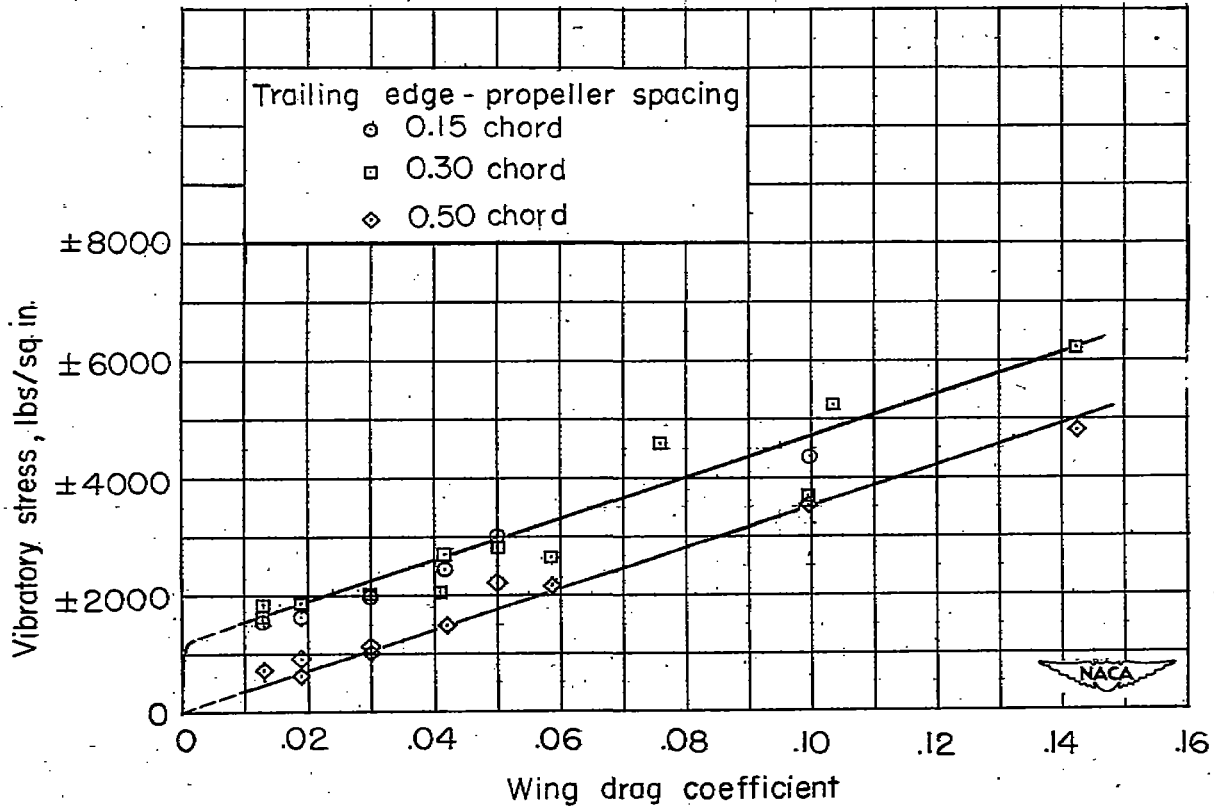


Figure 11.- Effect of velocity and of spacing between wing trailing edge and propeller disk upon peak vibratory stress. Flap deflection,  $0^\circ$ .



Balanced flap	0°	5°	10°	15°	20°				
Single split flap				13°	18°	13°	28°	18°	38°
Double split flap									

Figure 12.- Effect of drag coefficient and of spacing between wing trailing edge and propeller disk upon peak vibratory stress. Velocity, 150 miles per hour.

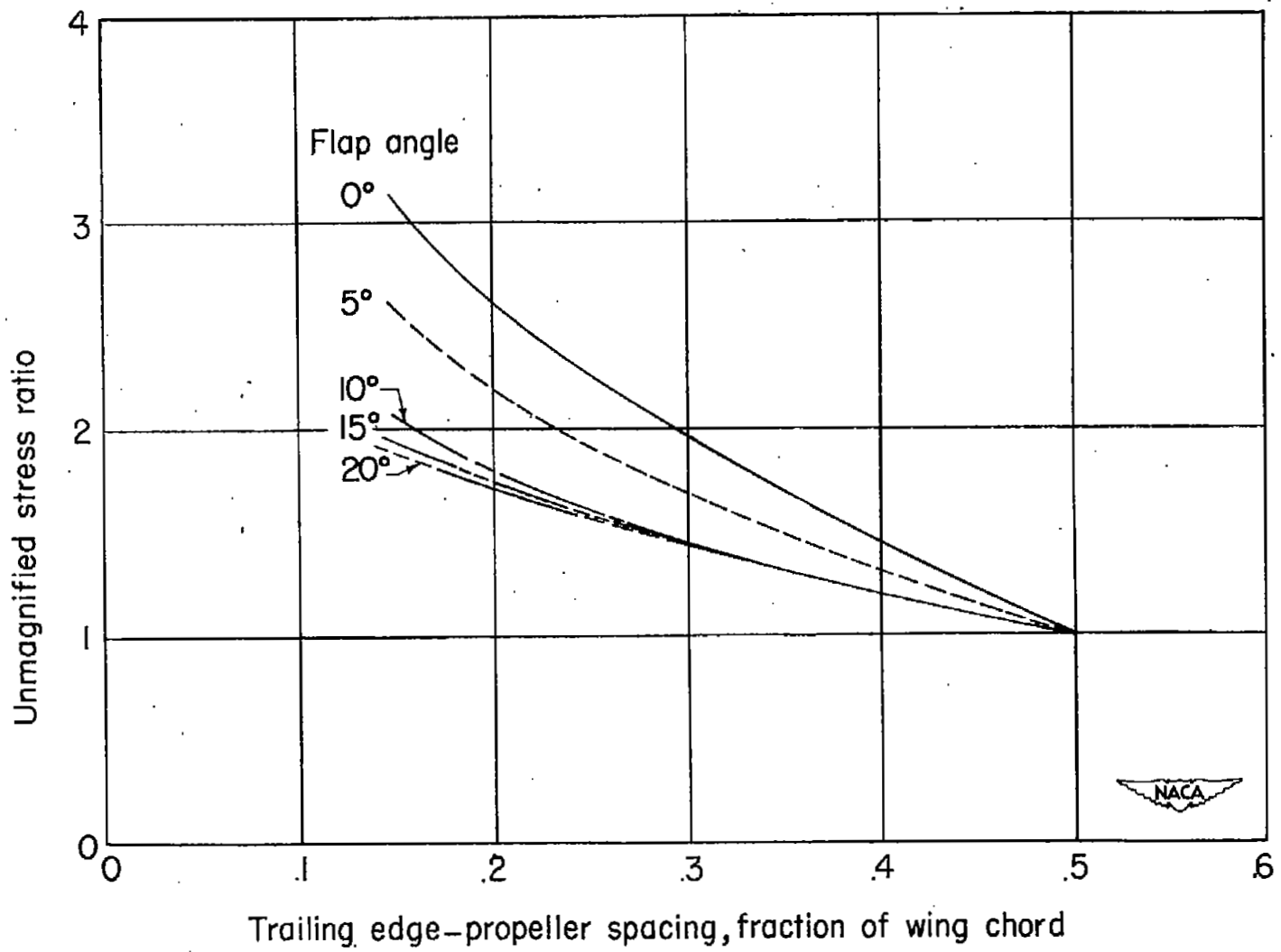


Figure 13.- Variation of unmagnified stress ratio with wing-propeller spacing. Balanced flap;  $V = 150$  miles per hour.



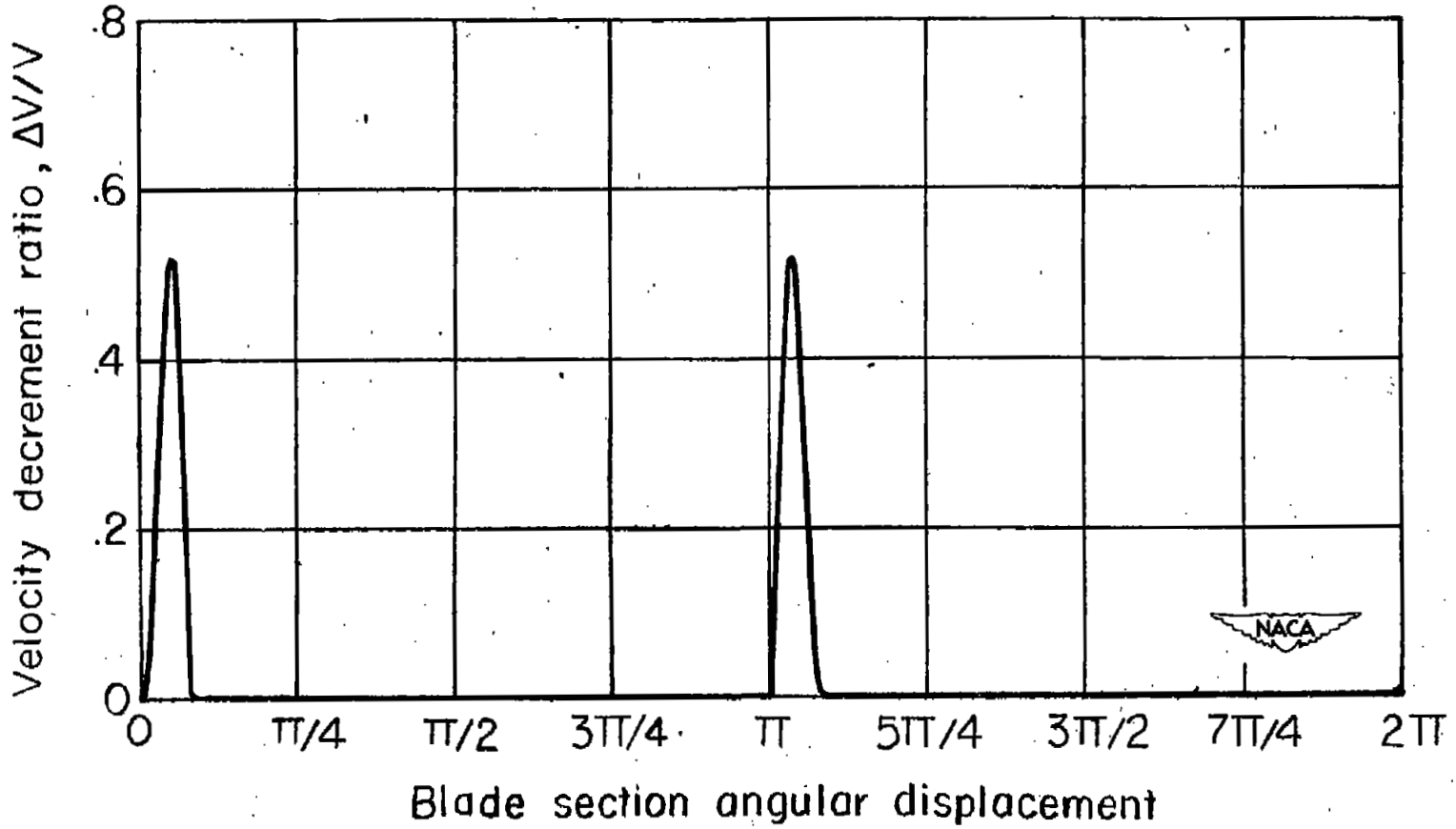


Figure 14.- Axial velocity cycle traversed by blade section at 0.7R behind balanced flap at  $5^\circ$  angle; spacing 0.50 chord;  $V = 150$  miles per hour.